



**Radiation Transport Effects in the Target
Chamber Gas of the Laser Fusion Power
Reactor SIRIUS-P**

J.J. MacFarlane, R.R. Peterson, P. Wang, G.A. Moses

May 1994

UWFDM-953

Prepared for the Eleventh Topical Meeting on the Technology of Fusion Energy, June
19–23, 1994, New Orleans LA.

FUSION TECHNOLOGY INSTITUTE

UNIVERSITY OF WISCONSIN

MADISON WISCONSIN

DISCLAIMER

This report was prepared as an account of work sponsored by an agency of the United States Government. Neither the United States Government, nor any agency thereof, nor any of their employees, makes any warranty, express or implied, or assumes any legal liability or responsibility for the accuracy, completeness, or usefulness of any information, apparatus, product, or process disclosed, or represents that its use would not infringe privately owned rights. Reference herein to any specific commercial product, process, or service by trade name, trademark, manufacturer, or otherwise, does not necessarily constitute or imply its endorsement, recommendation, or favoring by the United States Government or any agency thereof. The views and opinions of authors expressed herein do not necessarily state or reflect those of the United States Government or any agency thereof.

**Radiation Transport Effects in the Target
Chamber Gas of the Laser Fusion Power
Reactor SIRIUS-P**

J.J. MacFarlane, R.R. Peterson, P. Wang, G.A.
Moses

Fusion Technology Institute
University of Wisconsin
1500 Engineering Drive
Madison, WI 53706

<http://fti.neep.wisc.edu>

May 1994

UWFDM-953

Prepared for the Eleventh Topical Meeting on the Technology of Fusion Energy, June 19–23, 1994,
New Orleans LA.

RADIATION TRANSPORT EFFECTS IN THE TARGET CHAMBER GAS OF THE LASER FUSION POWER REACTOR SIRIUS-P

J. J. MacFarlane, R. R. Peterson, P. Wang, and G. A. Moses
Fusion Technology Institute, University of Wisconsin-Madison
1500 Johnson Drive
Madison, WI 53706-1687
(608) 263-6974

ABSTRACT

We present results from radiation-hydrodynamics calculations which show the central role resonant self-absorption plays in reducing radiative energy loss rates in high-gain ICF target chamber plasmas. Calculations were performed using a non-LTE radiative transfer model which we have recently coupled to our target chamber radiation-hydrodynamics code. The lower radiation fluxes escaping the plasma, which occur due to the self-absorption of line radiation in their optically thick cores, lead to significantly lower temperature increases at the surface of the target chamber first wall. The calculations were performed for the SIRIUS-P laser-driven direct-drive ICF power reactor. In this conceptual design study, high-gain targets release approximately 400 MJ of energy in the center of a gas-filled target chamber. The target debris ions and x-rays are stopped in the gas, and the energy is reradiated to the chamber wall over a much longer time scale. Because the time scales are comparable to the time it takes to thermally conduct energy away from the first surface, the thermal stresses and erosion rates for the first wall are greatly reduced.

I. INTRODUCTION

High-gain inertial confinement fusion (ICF) targets, such as those envisioned for ICF power reactors¹⁻⁵ or nearer-term test facilities,^{6,7} are expected to release $\sim 10^6 - 10^9$ joules of energy in the form of x-rays, energetic ions, and neutrons. Roughly two-thirds of the energy is emitted in the form of neutrons, which have long mean free paths and deposit their energy in the blanket surrounding the target chamber. The x-rays and target “debris” ions have relatively short mean free paths and deposit their energy in a much smaller volume of material

($\lesssim 10 \mu\text{m}$ at solid density). This can lead to serious problems for the target chamber wall, final optical components of the driver, diagnostic equipment, or any other material that is directly exposed to the target. Energy is released by the target over time scales $\sim 10^{-9} - 10^{-8}$ s, while the time it takes to conduct energy away from the surface is much longer ($\sim 10^{-6} - 10^{-5}$ s). This rapid deposition of energy onto exposed surfaces can lead to rapid temperature increases, large thermal stresses, and vaporization. Vaporization in particular can cause problems for the SIRIUS-P design because: (1) erosion rates can be excessive (which would require replacement of the first wall assembly), (2) the clearing time could limit the shot rate, and (3) the vapor could condense on laser optics.

One way to protect the target chamber first wall (FW), or any other optical or diagnostic component, is to fill the chamber with a low density buffer gas. The gas must have a sufficiently high density to stop the target x-rays and debris ions, but must have a low enough density to allow the laser beam to reach the target undegraded. The x-rays and ions then heat the buffer gas to high temperatures, and a significant fraction of the absorbed target energy is then reradiated to the FW over longer time scales. In addition, because higher temperatures and pressures are attained near the point of explosion, the plasma expands radially outward and can generate a strong shock. If the time scale over which energy is released by the buffer gas is comparable to or exceeds the time it takes to thermally conduct energy away from the thin absorbing FW surface layer, the potential problems associated with thermal stresses and vaporization can be avoided. It is therefore important to understand the time evolution of the hydrodynamic and radiative properties of the target chamber plasma.

The purpose of this paper is to assess the effects of line trapping — i.e., the self-absorption of line radiation in their optically thick cores — in reducing the radiation flux from the target chamber plasma. Target chamber plasmas have several attributes that make accurate modeling of their radiative properties somewhat difficult.^{8,9} First, the plasmas are line-dominated; that is, because of their moderately-low density ($n \sim 10^{16} - 10^{17}$ ions/cm³) their emissivity tends to be dominated by line radiation. Second, the plasmas are not in local thermodynamic equilibrium (LTE); thus, the atomic level populations are not readily obtained from the Saha equation and Boltzmann statistics. Photoexcitation effects are important and must be included in the atomic rate equations to obtain the non-LTE level populations. Third, the plasmas tend to be optically thick to line radiation, but can be optically thin to the continuum. The radiation field is not at all well-characterized by a Planck spectrum.

In the calculations discussed below, detailed radiative and atomic models are used to compute the radiative properties of the target chamber plasmas. The models are included within the target chamber radiation-hydrodynamics code, so that the atomic level populations and radiation field are computed self-consistently at each hydrodynamic time step. This is important because the time-dependent plasma conditions are very much affected by radiative energy losses. These calculations represent our first attempt to model the time-dependent radiative properties of ICF target chamber plasmas using detailed atomic and line radiation transport models within a radiation-hydrodynamics code. Our results indicate that resonant self-absorption has a major effect on reducing the flux at the chamber wall, thereby reducing potential problems associated with thermal stresses and vaporization.

II. THEORETICAL MODELS

The time-dependent plasma properties are computed using the CONRAD radiation-hydrodynamics code.¹⁰ This is a 1-D single-fluid Lagrangian radiation-hydrodynamics code, which includes models for the deposition of x-ray and ion energy from ICF target explosions. In the calculations discussed below, spherical symmetry is assumed. X-ray energy is deposited instantaneously in the buffer gas at the start of the calculation using “cold gas” photoabsorption cross sections.¹¹ The debris ion energy is deposited in the buffer gas using a multi-species stopping power model which includes the effect of free and bound elec-

trons on the stopping power.¹² The debris ions consist of C, He, H, D, and T. The ions are emitted isotropically and fully ionized from a point source. The location of each group of ions is tracked temporarily and spatially in a manner consistent with the energy deposition rate. The time-dependence of the mean ion charge state of each species is computed by solving atomic rate equations which include the effects of charge exchange.

Until recently, radiation transport in CONRAD was calculated using a multigroup diffusion model. However, it has been shown^{8,9,13} that multigroup diffusion models can significantly overestimate the radiation flux for plasmas with conditions typical of those in ICF target chambers (i.e., moderate density, line-dominated plasmas with optically thick lines and thin continuum). To overcome this, we have coupled a collisional-radiative equilibrium (CRE) model into CONRAD which transports the radiation of each line separately.¹⁴ In this model, atomic level populations are computed by solving multilevel statistical equilibrium equations self-consistently with the radiation field. The rates included in the model are: collisional excitation, deexcitation, ionization, and recombination; radiative and dielectronic recombination; and spontaneous decay and photoexcitation. Resonant self-absorption effects are included both in the determination of the level populations and in calculating the transport of line radiation energy throughout the plasma.

In the calculations discussed below, a hybrid radiation transport model was used. Continuum radiation was transported using the multigroup diffusion model, with multigroup opacities computed using IONMIX.¹⁵ Line radiation was transported using an angle- and frequency-averaged escape probability model.¹⁶ In this model, zone-to-zone coupling coefficients are used to compute the radiation flux and photoexcitation rates. The coupling coefficients are obtained from frequency-averaged escape probabilities for Voigt line profiles.

Calculations were performed for two plasmas: neon and xenon. The atomic model for Ne consisted of 108 atomic levels (configuration-averaged) distributed over all 11 ionization stages. For Xe, a total of 276 levels distributed over the lowest 30 ionization stages were used. It must be noted that while these calculations include considerably more detailed radiative and atomic models than previous calculations, the atomic model for Xe in particular must be considered to be only a rough approximation to the real atomic system. Because of the large num-

TABLE I

Target Yield and Chamber Parameters

Total target yield	400 MJ
Target x-ray yield	23 MJ
Target ion debris yield	84 MJ
Chamber radius	6.5 m
Chamber wall material	Graphite
Initial wall temperature	1,750 K

ber of bound electrons Xe can have ($Z = 54$), the atomic level structure is extremely complex. Energy levels, oscillator strengths, and photoionization cross-sections were generated from Hartree-Fock calculations. Additional details concerning the atomic physics models can be found elsewhere.¹⁷

III. RESULTS

Results are presented for two buffer gases which are thought to allow laser propagation at the given densities: 0.5 torr Xe ($n = 1.8 \times 10^{16}$ atoms/cm³) and 1.0 torr Ne ($n = 3.6 \times 10^{16}$ atoms/cm³). The advantage of Xe (which is the baseline case for SIRIUS-P) is that it can more efficiently absorb the target x-rays and debris ions before reaching the chamber wall. Ne, on the other hand, tends to radiate less (for the same plasma parameters) and is considerably easier to accurately model because of the fewer number of bound electrons. For both the Ne and Xe cases, 3 sets of calculations were performed to assess the effects of resonant self-absorption. In the first case, line radiation was transported using the CRE escape probability model, while the continuum (both bound-free and free-free radiation) was transported using multigroup diffusion. In the second case, both the line and continuum radiation were transported using the multigroup diffusion model. In the final case, line radiation was completely ignored in the calculation. In all cases, multigroup opacities were generated using IONMIX, with a total of 20 photon energy groups used. Table I lists the target yield and chamber parameters used in all calculations. Just over 100 MJ of energy is released by the target in the form of x-rays and energetic ions.

Results from the Ne buffer gas calculations are shown in Fig. 1, where the radiation flux at the FW, the time-integrated flux, and temperature at the FW surface are shown as a function of time after the target explosion. The solid curve on each plot corresponds to the calculation in which line radiation was transported using the CRE escape probability model. For comparison, results are also shown from calcu-

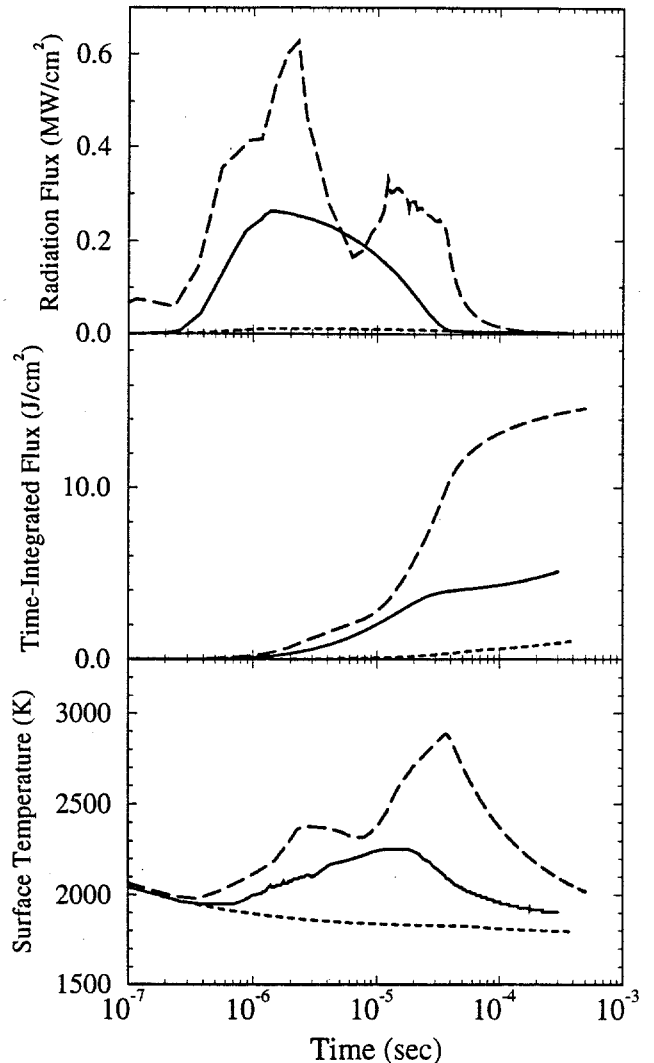


Fig. 1. Time-dependence of the radiation flux at the first wall (top), the time-integrated flux (middle), and temperature at the first wall surface (bottom) calculated for a Ne buffer gas. In each plot the CRE line transport calculations are indicated by the solid curves, while the multigroup diffusion results with and without line radiation are represented by the dashed and dotted curves, respectively.

lations with no line radiation (dotted curves) and line radiation included in the multigroup opacities of the diffusion model (dashed curves). It is clear that transporting the line radiation using the multigroup diffusion model leads to a significant overestimate of the radiation flux, and therefore temperature increase, at the FW. This occurs despite the fact that the line contributions to the multigroup opacities were computed using a much simpler atomic (hydrogenic ion) model,¹⁵ with a considerably less detailed line structure. The reasons multigroup diffusion models

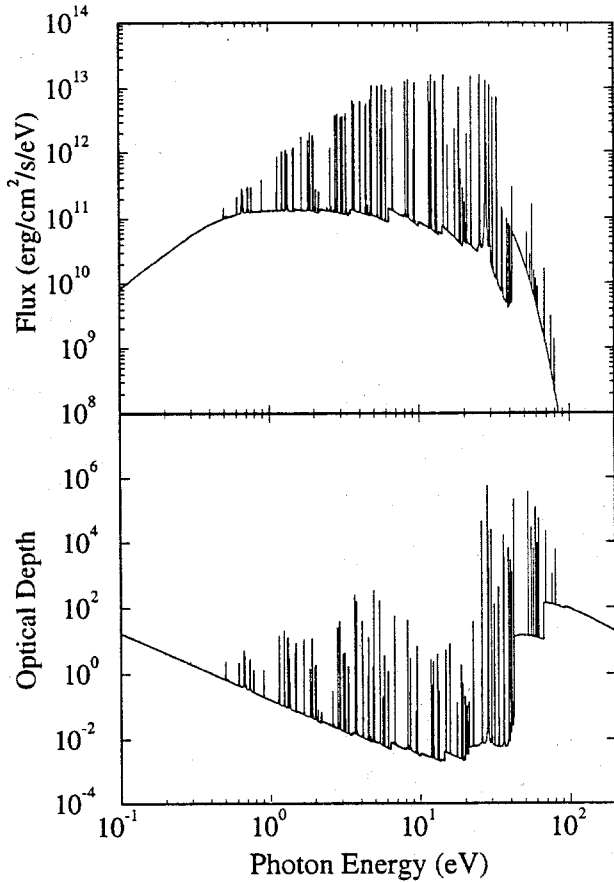


Fig. 2. Frequency-dependent flux (top) and optical depth (bottom) calculated at the boundary of a spherical Ne plasma at $T = 5$ eV, $n = 3.6 \times 10^{16}$ ions/cm³, and $R = 6.5$ m.

overestimate the radiation flux have been discussed at length elsewhere.^{8,9} The important point about Fig. 1 is that resonant self-absorption effects significantly reduce the radiation flux escaping the plasma, which keeps the temperature increase at the FW surface to an acceptable level (i.e., much below the vaporization temperature of graphite).

To more clearly illustrate the role of resonant self-absorption in ICF target chamber plasmas, Fig. 2 shows the calculated spectral flux emitted at the FW for an idealized Ne plasma at $T = 5$ eV, $n = 3.6 \times 10^{16}$ ions/cm³, and a radius of 6.5 m. Also shown (bottom) is the frequency dependent optical depth. Note that the optical depths of the strongest lines can be very large (up to $10^4 - 10^5$), while the continuum is optically thin ($\tau_\nu < 1$) between about 0.4 and 40 eV. Because of this, the flux in the line cores rises to near the Planck flux while the continuum flux is much below the Planck value.

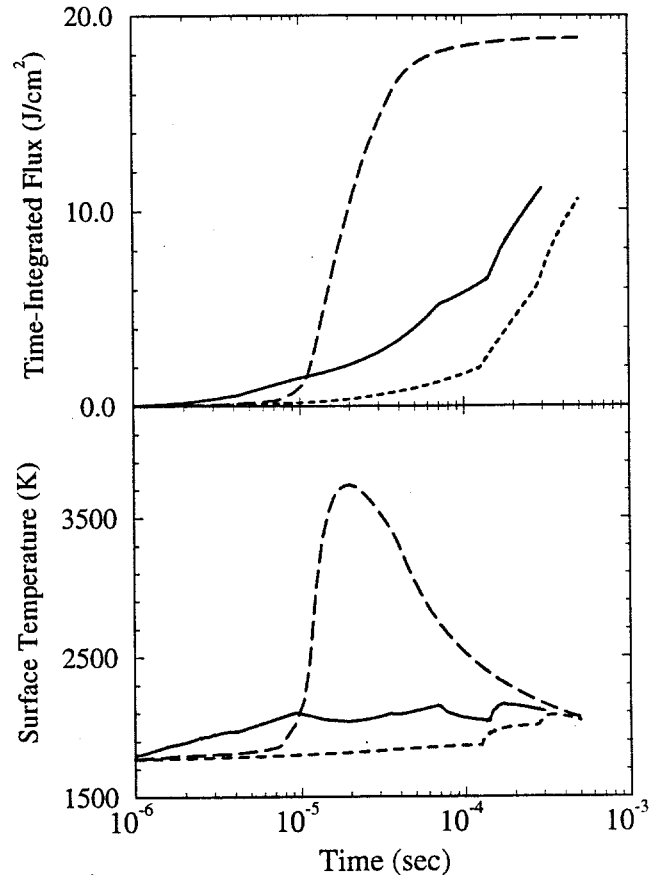


Fig. 3. Time-integrated radiation flux at the first wall (top), and temperature at the first wall surface (bottom) calculated for a Xe buffer gas. Curve definitions are the same at those in Fig. 1.

Results from radiation-hydrodynamics simulations for a Xe buffer gas are shown in Fig. 3, where the time-integrated flux and temperature rise at the FW are shown as a function of time. Again, it is seen that the calculations utilizing more detailed radiation and atomic physics models (solid curves) stretch out the time over which the absorbed target x-ray and ion energy is reradiated to the FW. Because of this, the temperature rise at the FW surface is only several hundred degrees, which is quite acceptable for graphite.

Our results indicate that both Xe and Ne buffer gases can effectively be utilized in ICF high-gain facilities to protect the FW and final laser optics from the target x-rays and debris ions. It is worth noting, however, that because of the complex processes involved in target chamber plasmas, particularly so for high-Z buffer gases such as Xe, experiments could provide valuable data which could lead to a significantly better understanding of the effects described in this

paper. Such experiments could be very similar to the laser-produced plasma experiments involving radiating moderate-temperature plasmas which have been performed in the past to study the evolution of blast waves.^{18,19}

ACKNOWLEDGEMENTS

This research has been supported in part by the U.S. Department of Energy.

REFERENCES

1. I. N. Sviatoslavsky, et al., "A Near Symmetrically Illuminated Direct Drive Laser Fusion Power Reactor-SIRIUS-P," these proceedings.
2. E. A. Mogahed, "Three-Dimensional Thermal and Structural Analysis of the First Wall in the SIRIUS-P Reactor," these proceedings.
3. R. W. Moir et al., "HYLIFE-II Inertial Fusion Energy Power Plant Design - Final Report," *Fusion Technol.*, **25**, 5 (January 1994).
4. G. A. Moses, et al., "Overview of the LIBRA Light Ion Beam Fusion Conceptual Design," *Fusion Technology*, **15**, 756 (1989).
5. B. Badger et al., "HIBALL-II - An Improved Conceptual Heavy Ion Beam Driven Fusion Reactor Study," Univ. of Wis. Fusion Tech. Inst. Report UWFD-625 (December 1984).
6. W. J. Hogan, "Missions and Design Requirements for a Laboratory Microfusion Facility," *Fusion Technology*, **15**, 541 (1989).
7. J. A. Paisner, "Introduction to the National Ignition Facility," Workshop on the Use of the National Ignition Facility for Inertial Fusion Energy Development, Berkeley, CA (February 1994).
8. J. J. MacFarlane and P. Wang, "Radiative Properties and Line Trapping Effects in Post-Explosion Inertial Fusion Plasmas," *Phys. Fluids*, **B3**, 3494 (1991).
9. J. J. MacFarlane, P. Wang, and G. A. Moses, "Implications of Non-LTE Buffer Gas Effects for ICF Target Chamber Design," *Fusion Technology*, **19**, 703 (1990).
10. R. R. Peterson, J. J. MacFarlane, and G. A. Moses, "CONRAD - A Combined Hydrodynamics - Condensation/Vaporization Computer Code," Univ. of Wis. Fusion Tech. Inst. Report UWFD-670 (July 1988).
11. F. Biggs and R. Lighthill, "Analytical Approximations for X-Ray Cross Sections III," Sandia National Laboratories Report SAND-0070 (August 1988).
12. T. A. Mehlhorn, "A Finite Material Temperature Model for Ion-Driven ICF Targets," *J. Appl. Phys.*, **52**, 6522 (1981).
13. G. A. Moses, R. R. Peterson, and J. J. MacFarlane, "Analysis and Experiments in Support of ICF Reactor Concepts," *Phys. Fluids*, **B3**, 2324 (1990).
14. J. J. MacFarlane, "Collisional-Radiative Equilibrium Model for the CONRAD Radiation-Hydrodynamics Code," Univ. of Wis. Fusion Tech. Inst. Report UWFD-937 (December 1993).
15. J. J. MacFarlane, "IONMIX - A Code for Computing the Equation of State and Radiative Properties of LTE and Non-LTE Plasmas," *Comp. Phys. Comm.*, **56**, 259 (1989).
16. J. A. Apruzese, et al., "Direct Solution of the Equation of Transfer Using Frequency- and Angle-Averaged Photon Escape Probabilities for Spherical and Cylindrical Geometries," *J. Quant. Spectrosc. Radiat. Transfer*, **25**, 419 (1981).
17. P. Wang, "Computation and Application of Atomic Data for Inertial Confinement Fusion Plasmas," Ph.D. Dissertation, Dept. of Nuclear Engr. and Engr. Physics, Univ. of Wis., Madison, WI (1991).
18. B. Ripin, et al., in *Laser Interactions and Related Plasma Phenomena*, Vol. 7, ed. H. Hora and G. H. Miley, p. 857, Plenum, New York (1986).
19. J. Grun, et al., "Instability of Taylor-Sedov Blast Waves Propagating Through a Uniform Gas," *Phys. Rev. Letters*, **66**, 2738 (1991).